Temperature Variation of the Photoinduced Birefringence of an Azo Dye Doped Polymer

P.-A. BLANCHE *and* PH. C. LEMAIRE

Centre Spatial de Liège (C.S.L.)
Université de Liège
Parc Scientifique du Sart Tilman
Avenue du Pré-Aily, B 4031 Angleur-Liège, Belgium

C. MAERTENS, P. DUBOIS, *and* R. JÉRÔME

Center for Education and Research on Macromolecules (C.E.R.M.)
Université de Liège
Sart Tilmant B6, B 4000 Liège, Belgium

The influence of the temperature on the photoinduced birefringence on an azo dye doped polymer film has been studied. Sample is composed of a polymer matrix PVK (Poly(N-vinylcarbazole)), doped with 10 weight percent (wt%) of the birefringent molecule DMNPAA (2,5-dimethyl-4-(p-nitrophenylazo)anisole) and 30 wt% of ECZ (N-ethylcarbazole) which acts as a plasticizer. Theoretical results can explain the behavior of the amplitude of the photoinduced birefringence versus temperature. Experimental and theoretical results are compared. Holographic recording experiments based on photoinduced birefringence have been carried out. Based on the effect of temperature, we have been able to significantly increase the diffraction efficiency of our sample.

1. INTRODUCTION

Polymer films doped with nonlinear organic molecules are, now, largely investigated for their potential applications in photonic devices such as data recording, wave length conversion, light amplification, optical computing, and so on (1–6). Consequently, the present studies are focused on the reversible holographic recording by photorefractivity or by photoinduced molecular orientational effect (5–8).

It is well known that photo-induced birefringence occurs in a doped polymer when birefringent molecules, originally randomly distributed, are aligned by electrical field of polarized light. Such a phenomenon can arise in azo dye doped polymer because the dye molecules can rotate by several photo-induced trans-cis isomerisations and cis-trans back-relaxation.

By using the photo-induced birefringence property, it is possible to write holograms. In such a case, the material records the polarization state of light instead of the intensity modulation (9). It is then important to understand the parameters that influence this process to improve the characteristics of this kind of recording medium.

The effects of the temperature on the mechanical properties of the polymers have been largely studied in the past but, until now, there are few works on its influence on optical properties (10, 11). Aiming a better understanding and optimization of the reversible influence of light on organic materials, we have analyzed the temperature effect on the photoinduced birefringence and the resulting holographic recording. Experiments developed in **Section 2** have shown that the amplitude and the time constant of these two phenomena dramatically increase when the temperature decreases.

In **Section 3**, theoretical results, derived from a new mathematical model describing the influence of the temperature on the amplitude of the photoinduced birefringence, are presented.

2. EXPERIMENTAL

Sample Preparation

Raw materials and chemical synthesis have been described elsewhere (7). Our samples have the following composition: the polymer matrix PVK (Poly(N-vinyl-

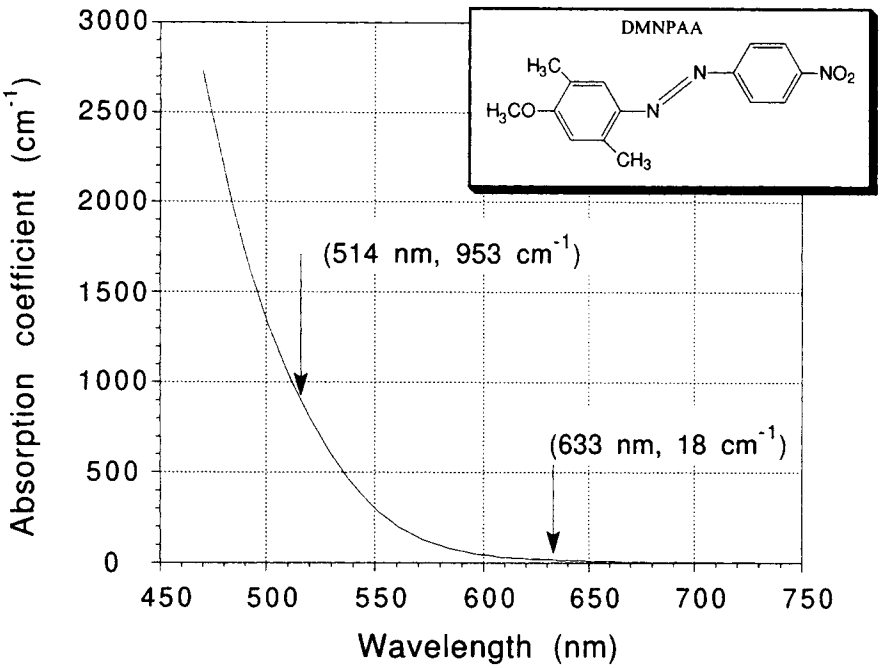

Fig. 1. Absorption coefficient spectrum of a 10 wt% DMNPAA doped PVK film with 30 wt% of ECZ. The absorption coefficient of the two wavelengths used for the experiments of this communication are indicated. Inlay: DMNPAA molecule representation.

carbazole)) has been doped with 10 wt% of the optically active molecule DMNPAA (representation: inlay into *Fig. 1* (2,5-dimethyl-4-(p-nitrophenylazo)anisole) and 30 wt% of ECZ (N-ethylcarbazole) which acts as a plasticizer. The glass temperature (T_g) of this compound, determined by Differential Scanning Calorimetry (DSC) was found to be around 10°C.

Film of PVK:DMNPAA:ECZ was prepared by dissolving the polymer and the doping molecules in tetrahydrofuran (THF). The solution was first filtered through a 0.5 μm filter and solvent was further evaporated under removed pressure in rotavapor (15 mm Hg). The resulting polymer was frozen to be easily crushed to a fine powder. This powder is placed on a glass plate between glass spacers, and heated at 140°C when the polymer begins to flow. A second glass plate is deposited above the other and pressed for 30 min to spread out the polymer. This operation provides a film with a good optical quality: homogeneous phase and coloration and no bubbles. The film thickness, measured by optical profilometry, is equal to the spacer thickness: 173 μm.

The absorption coefficient spectrum of the polymer film, recorded between 470 nm and 750 nm, is shown in *Fig. 1*. This result is similar to those presented by other authors (12).

Transmission Efficiency

The experimental setup is shown in the *Fig. 2*. A polarized argon beam (wavelength = 514 nm) is used to induce birefringence in the sample. We have fixed its intensity at 2.1 mW/cm^2 to avoid sample heating and to allow good quality measurements. A nearly parallel 633 nm HeNe laser beam is used as a probe to check the birefringence of the film. To avoid interference of the argon beam effect, the power of this beam has been set at 120 μW. The HeNe beam is polarized at 45° according to the argon beam polarization. After crossing the sample, it goes through an analyzer (tilted to 90° according to the initial HeNe polarization). A filter centered at 633 nm is placed in front of the detector to remove all the transmitted or scattered light coming from the argon laser.

The sample, positioned perpendicularly to the beams, is placed inside a vacuum chamber in order to avoid any condensation when the temperature decreases. Temperature is controlled by injecting liquid nitrogen in a cold trap attached to the sample support. A thermocouple fixed directly on the sample records the temperature.

We have recorded the transmitted power of the HeNe beam versus the time after the opening of the argon beam shutter for several temperatures of the sample. The transmission efficiency ($\eta_{transmission}$) is defined as the ratio between the transmitted and the incident powers of the HeNe beam. The experimental plots have been interpolated by *Eq 1*, which seems to be the best fit for this kind of measurement (11, 13). An example of measurement of the increase and decrease of the transmission efficiency is shown in *Fig. 3*.

$$\eta_{transmission} = A\left[1 - exp\left(\frac{-t}{\tau_A}\right)\right] + B\left[1 - exp\left(\frac{-t}{\tau_B}\right)\right] \quad (1)$$

The summation of the two parameters A and B gives the amplitude at saturation of the transmission efficiency. *Figure 4* shows the behavior of this sum ac-

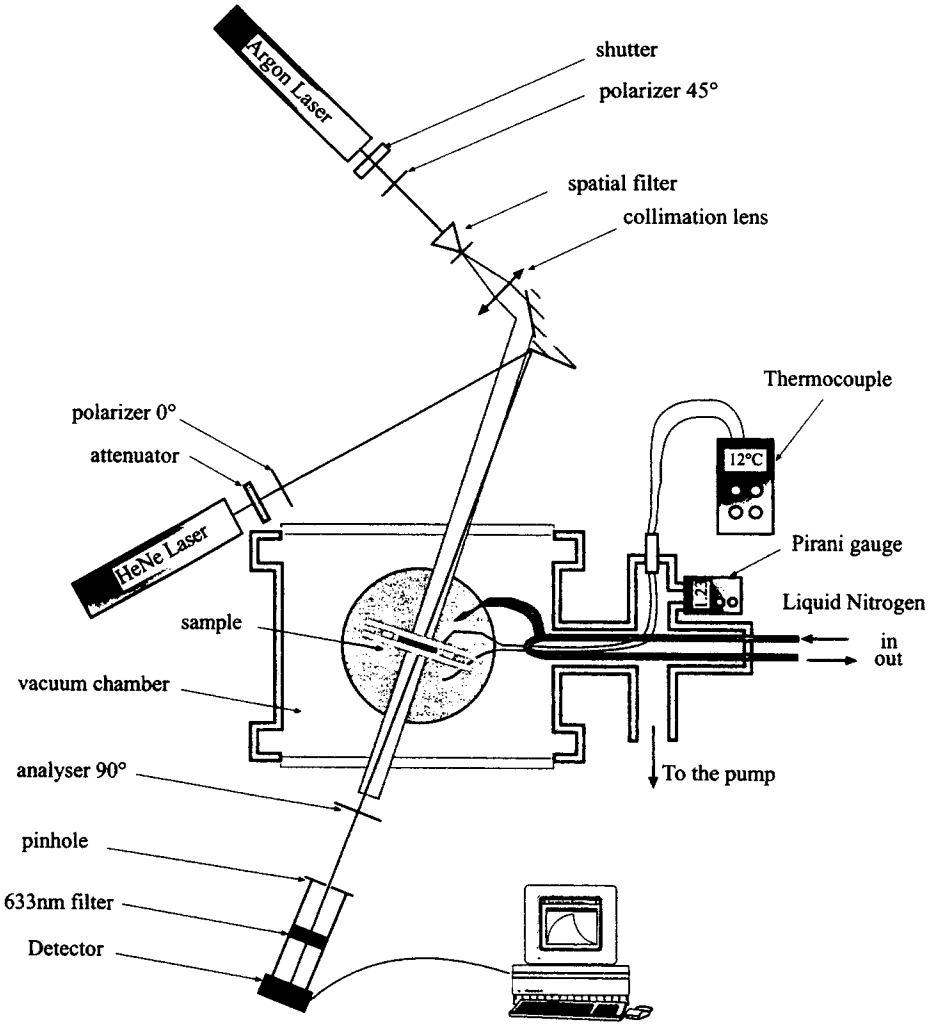

Fig. 2. Geometry of the experimental setup used for the photoinduced birefringence experiments.

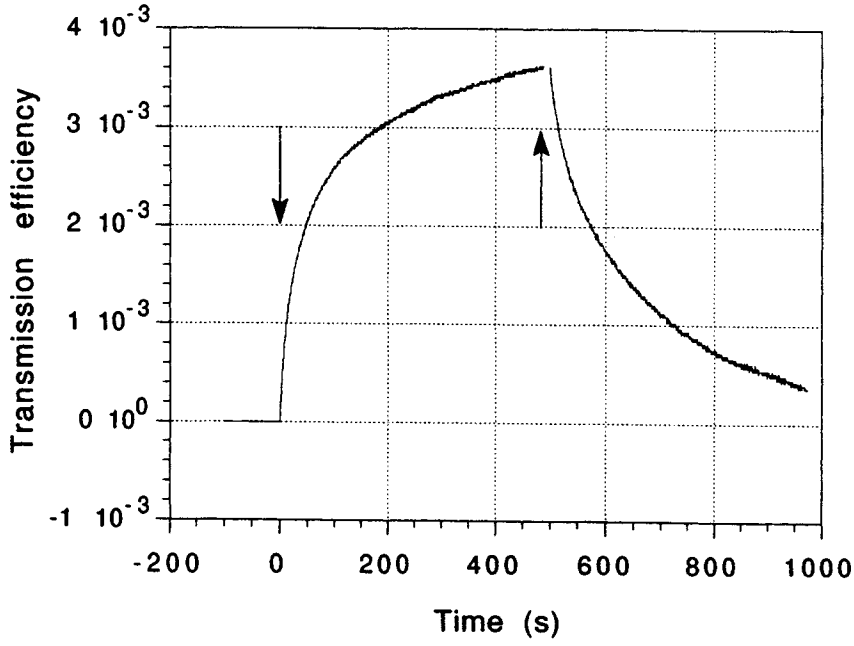

Fig. 3. Transmission efficiency of the HeNe beam. The arrows indicate the opening and the closure of the argon beam shutter.

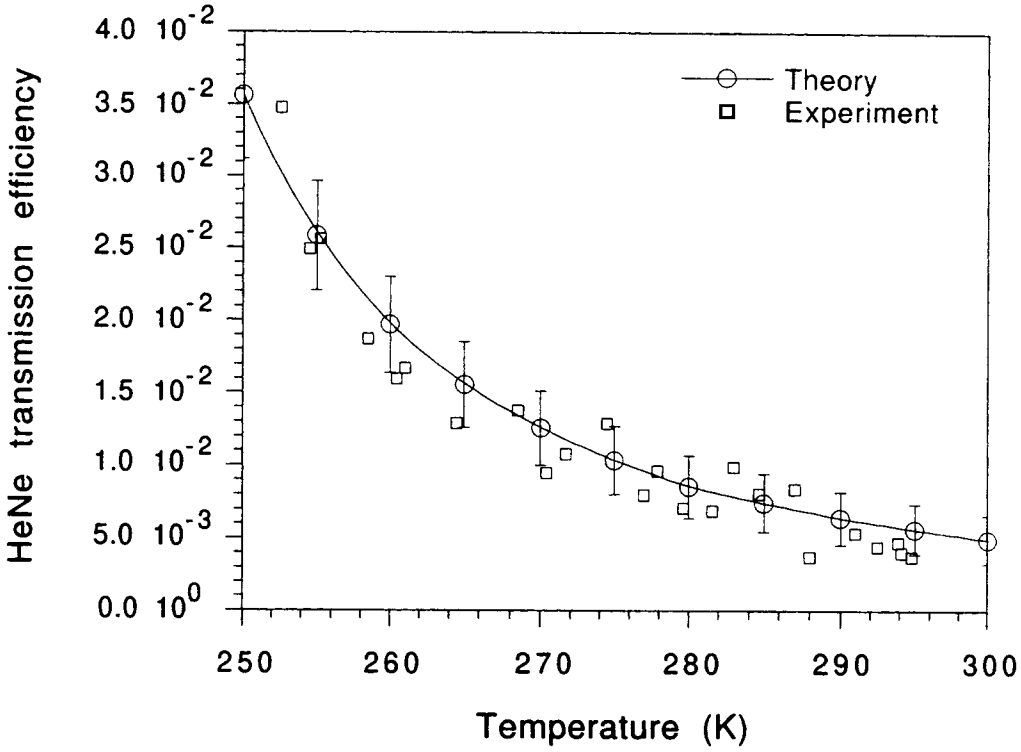

Fig. 4. Saturation amplitude of the transmission efficiency according to the temperature. Comparison of the experimental and theoretical plots. Parameters for the calculation are given in the text.

cording to the temperature. τ_A and τ_B are the two time constants of the phenomenon (called fast and slow, respectively).

It should be noticed that, even if the temperature range includes the polymer glass temperature (T_g = 10°C), there does not appear to be any difference in the behavior of the experimental plots: the birefringent molecules are still aligned in the argon beam field under the T_g. So, it does not seem very interesting to synthesize low T_g polymer in order to activate the orientationally enhanced photorefractive effect (14).

Diffraction Efficiency

In order to measure the diffraction efficiency, we have used the setup shown in *Fig. 5*. The 514 nm beam coming from an argon laser is split in two by a 50/50 beam splitter, the two resulting beams are filtered, expanded, and polarized vertically. Their intensities are 1.75 mW/cm^2 each. Both argon beams interfere in the sample by forming a 30° angle. A polarized HeNe beam is directed at the Bragg angle through the sample, and it is diffracted by the grating written by the argon beams. A detector, placed behind a filter whose transmitted bandwidth is centered on 633 nm, records to the diffracted intensity.

As for the photoinduced birefringence experiments, the sample is placed inside a vacuum chamber to avoid any condensation when the sample is cold. Its positioning is symmetrical according to the argon beam's angle. A cool trap supplied with liquid nitrogen cools the sample through a strap fixed on the sample holder. The cool trap is not directly in contact with the sample to avoid any vibration that will disturb the grating recording. A Michelson interferometer, with one arm reflecting itself on the sample, monitors the vibration of the sample. In this way, we can observe whether there is a mechanical vibration that will disturb the measurement or not.

By using this setup we have been able to record the diffraction efficiency of the HeNe beam versus the time after the opening of the argon beams shutter for the temperature range from 7°C to 22°C. It was not possible to decrease further the temperature of the sample because of thermal conversion of the argon light, which expands the polymer and prevents the recording of the grating. Measurements according to the angle between the polarization of the HeNe and the argon beams were also performed. *Figure 6* presents a typical measurement of diffraction efficiency versus time obtained with this setup.

The best curve fit that we have found for interpolating the diffraction efficiency according to the time is the one given by *Eq 2*. "a" is the saturation amplitude of the diffraction efficiency, and "$a.b$" is the original slope of the phenomenon.

$$\eta = \frac{a.b.t}{1 + b.t} \qquad (2)$$

By fitting our measurement, we have plotted the maximum of the increase of the diffraction efficiency

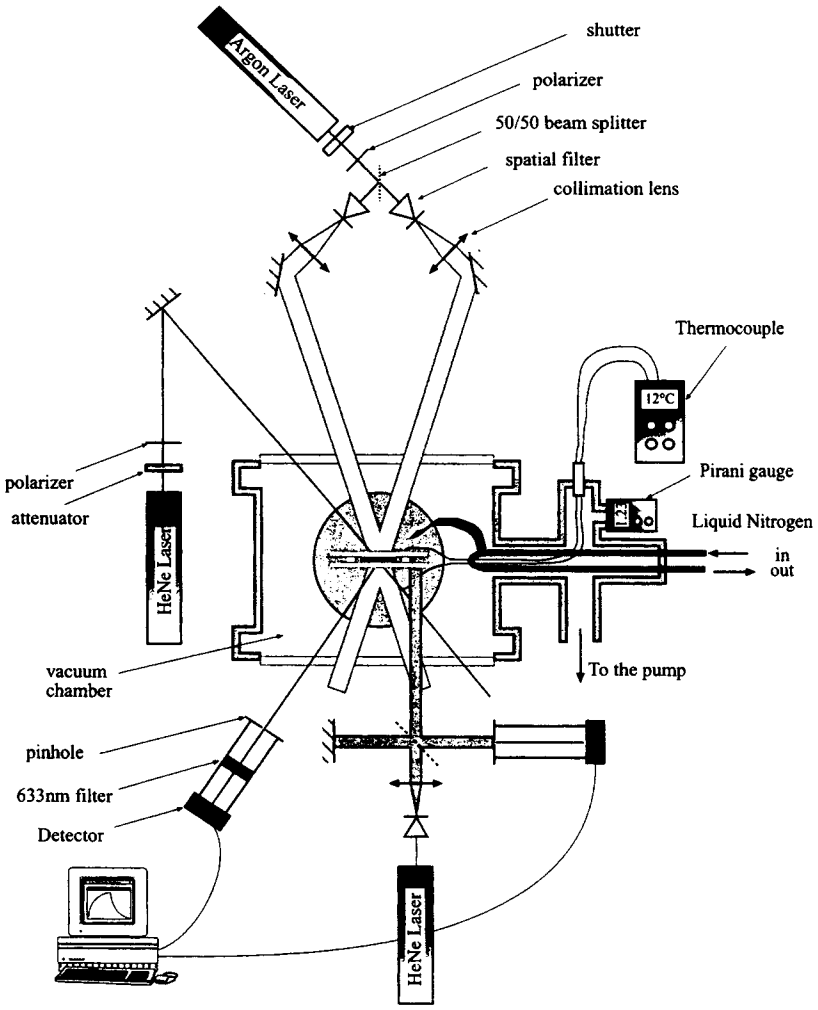

Fig. 5. Geometry of the experimental setup used for recording diffraction grating in the sample.

versus the temperature of the sample (*Fig. 7*). As already observed in the photoinduced birefringence, when the temperature decreases, the amplitude of the diffraction efficiency dramatically increases. We see that the diffraction efficiency can be increased by a factor higher than 2 by reducing the temperature of about 20°K. We are not surprised to find this similarity between holographic recording and the photoinduced birefringence since both these effects come from the same phenomenon: the molecular orientation.

3. THEORETICAL CALCULATION

In order to explain the behavior of the transmission efficiency amplitude versus temperature, we have developed a theoretical model based on statistical mechanics. In this model, it is assumed that the birefringent molecules are originally randomly orientated. Consequently, the sample is centrosymmetric, and no birefringence or phase grating can exist. When a polarized writing beam impinges the polymer film, the molecules tend to orientate themselves in such a way that the direction of their optical transition is perpendicular to the polarization direction of light. This induces a macroscopic refractive index change and birefringence (9). However, the thermal agitation counteracts the writing beam's action by disorganizing the symmetry, preventing all the molecules from being perfectly positioned.

Briefly, the theoretical model uses the Jones formalism to define each molecular layers of the sample, and its action on the electric field of the laser beam probe (*Eq 3*)

$$\begin{pmatrix} E'_x \\ E'_y \end{pmatrix} = \frac{1}{2}\begin{pmatrix} 1 & -1 \\ -1 & 1 \end{pmatrix}[R_{(-\varphi^N)} \cdot W_0^N \cdot R_{(\varphi^N)}] \ldots$$

$$[R_{(-\varphi^1)} \cdot W_0^1 \cdot R_{(\varphi^1)}] \cdot \frac{1}{\sqrt{2}}\begin{pmatrix} 1 \\ 1 \end{pmatrix} E \qquad (3)$$

E_i is the electric field along the i axis, $R_{(\varphi)}$ is the rotational matrix, with φ, the angle between the extraordinary index and the polarization axis of the HeNe beam; W_0, developed at *Eq 4*, represents the optical phase delay matrix; N is the number of layers used in the model:

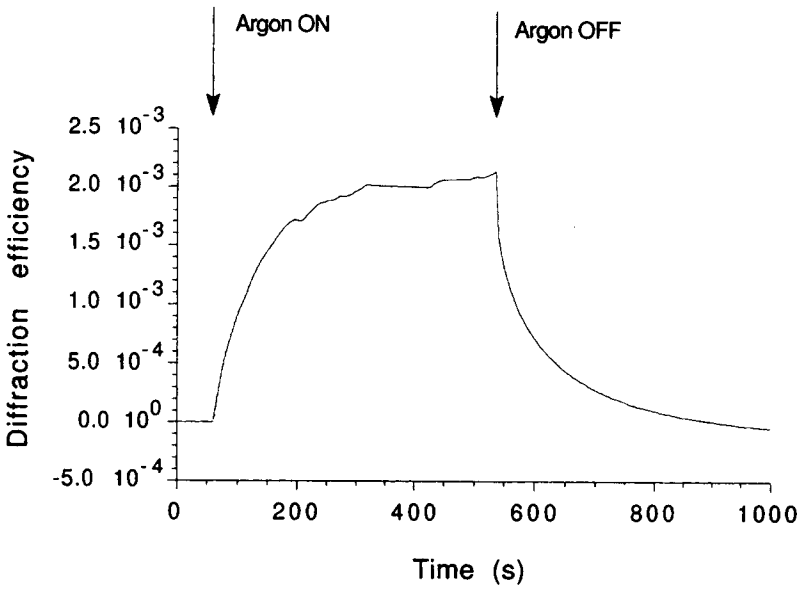

Fig. 6. Diffraction efficiency according to the time. The arrows indicate the opening and the closure of the argon beam shutter. The temperature was 22.7°C. Writing intensity 2 × 1.75 mW/cm². Writing beam ratio: 1/1. Angle between writing beam: 50°, symmetrical configuration. HeNe beam power: 140 μW.

$$W_0 = \begin{pmatrix} e^{-i\Gamma/2} & 0 \\ 0 & e^{i\Gamma/2} \end{pmatrix} \text{ with } \Gamma = \frac{2\pi}{\lambda} d(n_o - n_e(\theta)) \quad (4)$$

where λ is the wavelength of the HeNe beam, d is the thickness of the molecular layer, n_o is the normal refractive index, $n_e(\theta)$ the extraordinary refractive index depending on the angle θ between the molecular axis and the beam propagation direction.

The transmitted efficiency ($\eta_{transmission}$) is given by *Eq 5*, where $I_{incident}$ is the intensity incident to the sample.

$$\eta_{transmission} = \frac{(E'_x\ E'_y)\cdot\begin{pmatrix} E'^*_x \\ E'^*_x \end{pmatrix}}{I_{incident}} \quad (5)$$

Each birefringent molecule has a fixed direction depending on the argon beam polarization and intensity, and on the thermal agitation. Thus, all the matrices in *Eq 3* are different: $R_{(\varphi)}$ by the angle φ and the W_0 by θ.

Moreover, there is no relation between the direction of the molecule and its position in the sample, as it is the case for the liquid crystals. So, it is not possible to reduce the number of matrices representing the optical system. The number $nb_{(\theta_1)}$ of molecules orientated at the angle θ_1 in the sample can be found from statistical mechanics. It is given by *Eq 6*, where A is a parameter depending on various molecular constants (cross section, dipolar momentum, ...), ε represents the amplitude of the electrical field of the argon beam and θ_1 is the angle between the molecular optical axis and the argon polarization axis. T_0 is a temperature threshold: at this limit, all the molecules are aligned, decreasing the temperature further does not influence the molecular orientation anymore.

$$nb_{(\theta_1)} = \frac{Ne^{\frac{-A\,\varepsilon\,\cos^2(\theta_1)}{k(T-T_0)}}}{\int_0^{\pi} e^{\frac{-A\,\varepsilon\,\cos^2(\theta_1)}{k(T-T_0)}} \frac{\sin(\theta_1)}{2}\, d\theta_1} \frac{\sin(\theta_1)}{2} \quad (6)$$

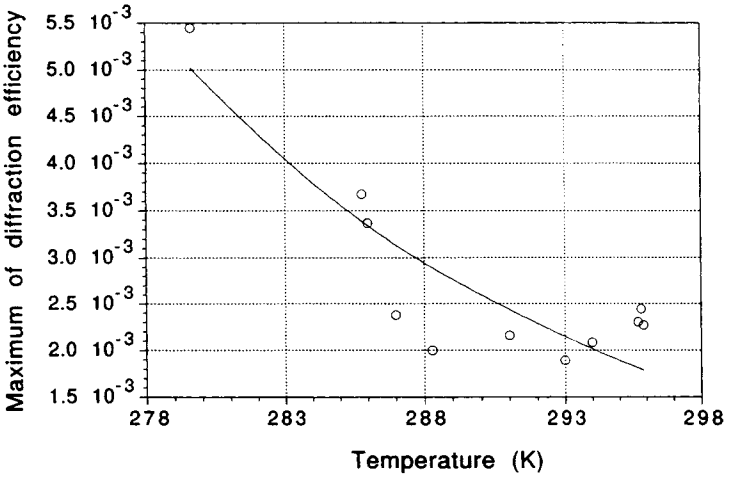

Fig. 7. Maximum of diffraction efficiency versus temperature of the sample. The fit is only a guide for the eyes.

The knowledge of θ_1 allows us to determine φ and W_0 of *Eq 3* for each molecule on the optical path. For a sequence of molecules whose statistical angular distribution of θ_1 is given by *Eq 6*, we are able to calculate the transmission efficiency versus temperature.

We have not found an analytical solution for the transmission efficiency versus sample temperature. However, it is possible to carry out a numerical calculation to display its behavior; the results are shown at *Fig. 4*. For this simulation, we have fixed the number of layers at 7000. The parameter $A.\varepsilon/k$ has been determined to be equal to 9 K and the threshold temperature to be T_0 = 222 K. The ordinary and extraordinary indexes have been set to n_o = 1.6, n_e = 1.62, and the thickness of the molecular layer is equal to the sample thickness divided by the number of layers d = 173/7000 μm. The plot in *Fig. 4* is the average of ten simulations, and the error bar's length is twice the standard deviation. The theoretical curve seems to be in good agreement with the experimental plots.

The set of parameters introduced in the numerical calculation has been chosen to fit the experimental curve. However, it will be interesting to measure the transmission efficiency at lower temperature in order to test the theoretical model and to refine the parameters. We have noticed that A and n_o-n_e have nearly the same action on the theoretical curve shape; an independent measurement of n_o-n_e of the active molecules will allow us to set A more precisely.

4. CONCLUSIONS

According to our experimental measurements, carried out on a PVK:DMNPAA:ECZ (74:10:16 % wt) polymer film, the temperature of the sample reveals itself to be an important parameter for the photoinduced birefringence and for the diffraction efficiency: we have noticed that temperature dramatically influences the amplitude of both the photoinduced birefringence and the diffraction efficiency. The lower the temperature, the higher the amplitude of these two measurements. To our best knowledge this is the first report of this behavior. The temperature ranges from −20°C to 22°C; so it includes the T_g of the sample (10°C); however, no modification of the polymer behavior appears before or after this point.

In addition to the experiments, we have proposed a mathematical model in order to explain the influence of the temperature on the photoinduced birefringence. The theoretical plots are in good agreement with the experimental ones. Parameters introduced in the numerical calculation have been set only to fit the experimental plots; further measurements will be interesting in order to refine and to compare them with physical coefficients.

REFERENCES

1. P. M. Lundquist, R. Wortmann, C. Geletneky, R. J. Twieg, M. Jurich, V. Y. Lee, C. R. Moylan, and D. M. Burland, *Science*, **274**, 1182 (1996).
2. J. Xu, G. Zhang, Q. Wu, Y. Liang, S. Liu, X. Chen, and Y. Shen, *Optics letters*, **20**, 504 (1995).
3. S. V. O'Leary, *Optics Communications*, **104**, 245 (1994).
4. L. R. Dalton, A. W. Harper, B. Wu, R. Ghosn, J. Laquindanum, Z. Liang, A. Hubble, and C. Xu, *Advanced Materials*, **7**, 519 (1995).
5. B. Volodin, B. Kippelen, K. Meerholz, N. Perghambarian, N. V. Kukhtarev, and H. J. Caulfield, *J. Optical Society of America B*, **13**, 2261 (1996).
6. P. M. Lundquist, C. Poga, R. G. DeVoe, Y. Jia, W. E. Moerner, M.-P. Bernal, H. Coufal, R. K. Grygier, J. A. Hoffnagle, C. M. Jeffersonj, R. M. Macfarlane, R. M. Shelby, and G. T. Sicerbox, *Optics Letters*, **21**, 890 (1996).
7. P.-A. Blanche, Ph.C. Lemaire, C. Maertens, P. Dubois, and R. Jérôme, *Optics Communications*, **139**, 92 (1997).
8. W. Chalupczak, C. Fiorini, F. Charra, J.-M. Nunzi, and P. Raimond, *Optics communications*, **126**, 103 (1996).
9. T. Todorov, L. Nokolova, and N. Tomova, *Applied Optics*, **23**, 4309 (1984).
10. S. Ivanov, I. Yakovlev, S. Kostromin, and V. Shibaev, *Makromolecular Chemistry, Rapid Communication*, **12**, 709 (1991).
11. J. S. Hwang, G. J. Lee, and T. K. Lim, *J. Korean Physical Society*, **27**, 392 (1994).
12. B. L. Volodin, Sandalphon, K. Meerholz, B. Kippelen, N. V. Kukhtarev, and N. Peyghambarian, *Optical Engineering*, **34**, 2213 (1995).
13. M. S. Ho, A. Natansohn, and P. Rochon, *Macromolecules*, **28**, 6124 (1995).
14. W. E. Moerner, S. M. Silence, F. Hache, and G. C. Bjorklund, *J. Society of America B*, **11**, 320 (1994).